 doi:10.20944/preprints202105.0667.v1

Article

Crushing of Double-Walled Corrugated Board and its Influence on the Load Capacity of Various Boxes

Tomasz Gajewski [1,*], Tomasz Garbowski [2], Natalia Staszak [3] and Małgorzata Kuca [4]

[1] Institute of Structural Analysis, Poznan University of Technology, Piotrowo 5, 60-965 Poznań, Poland
[2] Department of Biosystems Engineering, Poznan University of Life Sciences, Wojska Polskiego 50, 60-627 Poznań, Poland; tomasz.garbowski@up.poznan.pl (T.G.)
[3] Reserach and Development Department, FEMat Sp. z o.o., Romana Maya 1, 61-371 Poznań, Poland; natalia.staszak@fematproject.pl (N.S.)
[4] Schumacher Packaging Sp. z o.o., Wrocławska 66, 55-330 Krępice, Poland; malgorzta.kuca@shumacher-packaging.com.pl (M.K.)
* Correspondence: tomasz.gajewski@put.poznan.pl

Abstract: As long as the non-contact digital printing is not a common standard in the corrugated packaging industry, corrugated board crushing is a real issue that affects the load capacity of the boxes. Crushing mainly occurs during the converting of corrugated board (e.g. analog flexographic printing or laminating) and is a process that cannot be avoided. However, as show in this study, it can be controlled. In this work, extended laboratory tests were carried out on the crushing of double-walled corrugated board. The influence of fully controlled crushing (with a precision: $\pm 10\ \mu m$) in the range from 10 to 70 % on different laboratory measurements was checked. Most of the typical mechanical tests were performed e.g. edge crush test, four-point bending test, shear stiffness test, torsional stiffness test, etc. on reference and crushed specimens. The residual thickness reduction of the crushed samples was also controlled. All empirical observations and performed measurements were the basis for building an analytical model of crushed corrugated board. The proven and verified model was then used to study the crushing effect of the selected corrugated board on the efficiency of simple packages with various dimensions.

Keywords: corrugated cardboard; converting; crushing; numerical homogenization; strain energy equivalence; finite element method; shell structures; transverse shear

1. Introduction

Corrugated cardboard packaging is one of the most common way to protect various goods during storage, transportation and delivery or shop exposition. Current trend in developed and middle developed countries is consuming various goods, from household products through food, clothing to automotive elements, etc. Thus, the corrugated cardboard packaging is growing in popularity and application. The packaging must be tailored for particular good, i.e. adequate geometry and strength, also sometimes with additional features, such as holes [1,2], perforations [3], specific shape [4], inserts/dividers or locking tabs.

The double wall corrugated boards considered in this study are used in large-size collective packaging for products with a large mass which must protect the goods from accidental mechanical damage and/or withstand the product large mass. Often, to elevate the corrugated board packaging the kraftliner type of papers are used for boards, those papers, on contrary to the testliner papers, have small amount of recycled fibres. The products packed with boxes using double-wall corrugated cardboards are electrical household appliances, such as TVs, washing machines fridges, furniture components. Also, some more fragile elements such as, glass bottles, wines, perfumes or auto parts, such as bonnet, bumpers are protected by those boards. Depending on the application, the outer layer may be natural or one/two white side. The double wall boards are created

 doi:10.20944/preprints202105.0667.v1

from five paperboards, three liners (flat layers) and two fluting layers. The most common composition for double walls are formed from BC (5 − 7 mm), EB (3.5 − 5 mm) or EC (4 − 5.5 mm) flutes. The grammage of the corrugated boards are usually 550 − 900 g/mm^2, but also 480 or 1300 g/mm^2 may be found in the market.

Double wall corrugated cardboards are used from many years to design packaging [5]. The analytical methods to determine the packaging strength do not differentiate between single or double wall cases [6–10]. Those methods take into consideration selected mechanical properties of the cardboard derived in the mechanical tests, such as edge crush test (ECT) [11] or torsion test [12,13]. Thus, the analytical methods, those simplified, such as the most know McKee formula [**Error! Bookmark not defined.**] and more advanced, such as our recently published one [**Error! Bookmark not defined.**], may be used to estimate the box compression test (BCT) output. This advanced approach takes into consideration the transverse shear stiffness [12–15], what seems significantly important to be included in estimating the strength for converted cardboards, as shown in our recent paper [16].

In converting processes, i.e. printing, lamination or die-cutting etc., the crushing of the corrugated cardboard is observed. If the crushing is severe, the delamination of the paper of fluting would appear, as presented in [17]. In single wall corrugated boards, the fluting shape transforms to a characteristic trapezoidal form, like shown in experimental [**Error! Bookmark not defined.**,18] and numerical [**Error! Bookmark not defined.**] studies. According to our knowledge, in double wall corrugated boards, the crushing was not studied. Since the elevated strength is crucial in double-walled corrugated boards, the crushing effect, cannot be neglected to ensure the proper strength specification of the packaging.

As discussed above, the crushing effect significantly decreases the mechanical properties in single wall corrugated cardboards [16**Error! Bookmark not defined.**]. The decrease in ECT index of corrugated board is small due to preserving the material area, which in most influences the ECT index [**Error! Bookmark not defined.**]. In torsion or bending, the stiffness decrease is more severe due to crushing, since the cardboard quickly recovers its crushed geometry (trapezoidal form like). The more the trapezoidal form the more decrease of thickness is achieved. Decreased thickness due to a small moment of inertia causes such high sensitivity of torsion and bending to crushing. The above discussion seems straightforward and clear for single wall corrugated cardboards, but for double wall cardboard some additional issues may appear. For instance related with different fluting periods of two flutings, thus, a local in-span bending of internal liner; or more complex shape due to crushing, than simple trapezoidal form, like the one in crushing of single wall boards. Those effects have not been studied in the literature, but in corrugated cardboard processing is known from few years.

From the concept of industry 4.0 point of view, the information of crushing of the cardboard material during production due to different technological processes would raise the quality control on much higher level. The optimal solutions and savings on the box designs are available due to advanced mathematical modelling, this may be related with a single box feature [**Error! Bookmark not defined.**,**Error! Bookmark not defined.**] or with more heuristic approach to design [19,20]. Currently, the practitioners know that crushed material is weaker, but does not have the techniques/tools/models to measure how much and which technological process is the most crucial here. Thus, this paper verifies which typical, mechanical tests of corrugated cardboard have the biggest potential to identify the crushing level through series of experimental tests of corrugated cardboards samples, but using the samples with induced level of crushing. Moreover, it has been numerically demonstrated what is the decrease of packaging performance if the particular level of crushing was obtained in double-walled boards and how significant this effect is. The results obtained and experimental observations may serve as a guide for

 doi:10.20944/preprints202105.0667.v1

designers of packaging with analogue prints or laminated boxes, and the proposed analytical model of crushed corrugated board may be used to better predict the load capacity of ecological packages.

 doi:10.20944/preprints202105.0667.v1

2. Materials and Methods

2. 1. Mechanical tests of corrugated cardboard

Various tests can be conducted to determine the stiffness and strength of a corrugated board. The mechanical tests often performed in cardboard packaging laboratories are: (a) stiffness in the four-point bending test – BNT, (b) edge crush test – ECT, (c) shear stiffness testing – SST and (d) torsional stiffness test – TST. All these test can be done on a single laboratory machine called BSE System from Femat [21].

The four-point bending method (BNT) is a laboratory test in which the bending stiffness is measured, see Figure 1. Samples of 50 × 250 millimeters are usually used for this kind of tests. Due to static scheme of the specimen a constant moment and zero shear force between the internal supports are obtained. As a result, the influence of transverse shear stiffness on the half-span deflection of the sample can be eliminated and the results of bending stiffness are more accurate. Shear force is still present between the outer and inner supports. Sample damage (fracture and/or crushing) has a large impact on the bending stiffness measurement. Thus, for samples with more than 50% crushing, the results are unreliable.

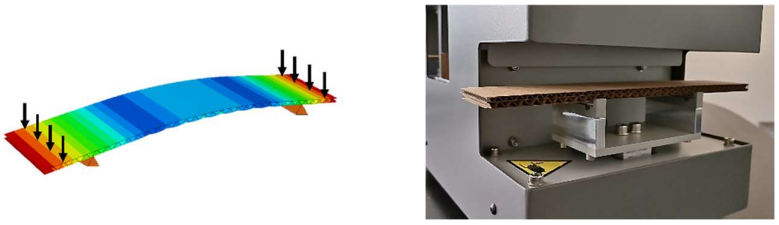

(**a**) (**b**)

Figure 1. The four-point bending test - BNT: (a) loaded and deformed specimen; (b) cardboard testing device.

The compressive strength of the specimen is determined in Edge Crush Test (ECT), see Figure 2. The ECT is one of the most important and recognizable parameter of corrugated board from a practical point of view. The test is carried out on specimens of 25 ×100 millimeters and usually thicker than 1 millimeter. Note that while testing slender sample (e.g. corrugated board with E and F flute), loss of stability is it primary failure mechanism, and not, as the name of test suggests – crushing of a specimen.

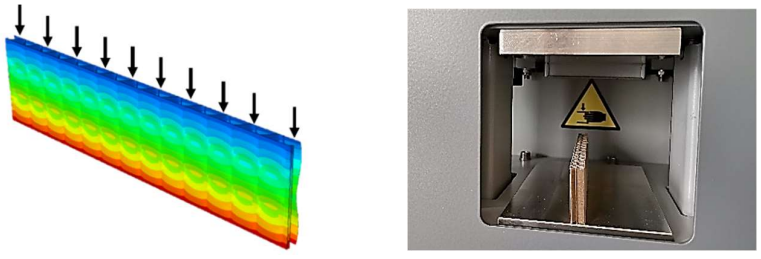

(**a**) (**b**)

Figure 2. The edge crush test - ECT: (a) loaded and deformed specimen; (b) cardboard testing device.

The measurement of the shear stiffness (SST) of corrugated board is conducted by twisting a sample with dimensions of 80 × 80 millimeters with a pair of forces, see Figure 3. During the test the a known displacement is applied at two corners of a rectangular sample (two points on the diagonal) and the displacements at the other two corners is measured. It allows to determine the shear stiffness of the cardboard. Only the linear load-

 doi:10.20944/preprints202105.0667.v1

displacement relationship is used to determine the stiffness of the sample. Crushing of the sample, i.e. thickness reduction, has a significant effect on the SST parameter.

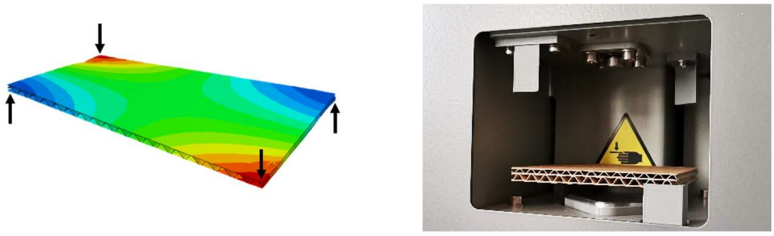

(**a**) (**b**)

Figure 3. The shear stiffness testing - SST: (a) loaded and deformed specimen; (b) cardboard testing device.

The torsional stiffness test (TST) is based on twisting a samples of 25 × 150 millimeters by a few degrees in both directions, see Figure 4. Only the linear part of a curve describing the angle of rotation with respect to the bending moment is used to specify the torsional stiffness of the specimen. The guarantee of reliable results are: (i) a static method of measuring the angle of torque and rotation, (ii) a stable method of holding the specimen, and (iii) a relatively large width of the sample. Reliable results in TST are obtained even for very deteriorated and crushed specimens.

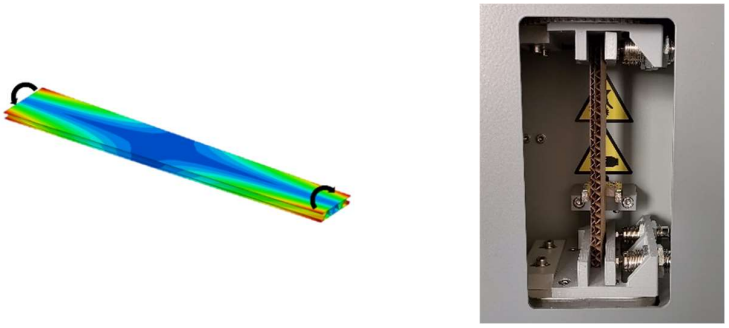

(**a**) (**b**)

Figure 4. The torsional stiffness test - TST: (a) loaded and deformed specimen; (b) cardboard testing device.

The CRS (crushing device from Femat [22]) is used to evaluate the influence of processes such as stamping, laminating and analogue printing or creasing on the load capacity and quality of corrugated board or packaging, see Figure 5. Cardboard crushing can be performed with a laboratory machine CRS in a fully controlled manner in the range from 10% to 70%.

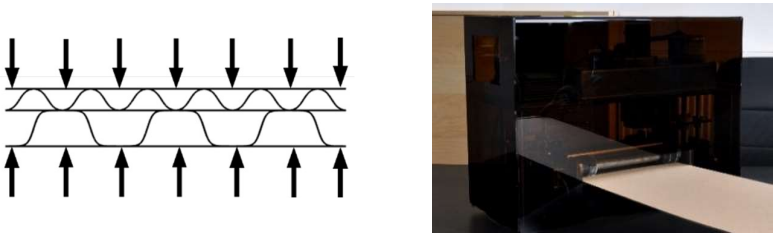

(**a**) (**b**)

Figure 5. The cardboard crushing - CRS: (a) loaded and deformed specimen; (b) cardboard testing device.

 doi:10.20944/preprints202105.0667.v1

2.2. Coefficient of determination and estimation error

To understand the impact of the crushing of corrugated board on the various mechanical properties measured in different tests, first the correlation between the level of crush and the decrease in the individual measured quantities was investigated. The coefficient of determination R^2 was calculated for each index of cardboard to determine the relationship between the crushing and decrease of the stiffness value of the corrugated board according to the formula:

$$R^2 = 1 - \frac{\sum_{i=1}^{n}(x_i - \hat{y}_i)^2}{(n-1)\cdot \mathrm{var}(x)}, \tag{1}$$

where: x_i – the expected ratio of the measured value of the crushed sample to the initial value of measured parameter ($\mathrm{CRS} = 0\% \rightarrow x_i = 1.0, \mathrm{CRS} = 10\% \rightarrow x_i = 0.9$, etc.), $\hat{y}_i$ – the values computed on the basis of the Equation (2) describing the linear regression, $\mathrm{var}(x)$ – the variance of the expected ratio of the measured value of the crushed sample to the initial value,

$$\hat{y}_i = \bar{a}(x_i - \bar{x}) + \bar{y}, \tag{2}$$

where: $\bar{x}$ – the mean value of the expected ratio of the measured value of the crushed sample to the initial value, $\bar{y}$ – the mean value of the measured quantity (e.g. SST-MD, TST-CD etc.). Parameter $\bar{a}$ is the slope of the linear regression:

$$\bar{a} = \frac{\sum_{i=1}^{n}(x_i - \bar{x})(y_i - \bar{y})}{\sum_{i=1}^{n}(x_i - \bar{x})^2}. \tag{3}$$

2.3 Numerical-analytical approach for modelling crushing

In this study, not only laboratory measurements were performed, also the extended numerical computations of double-walled packaging compressive strength were conducted including different levels of crushing. In computations, a similar workflow was used, like in [16], however, it should be noted that the crushing shape was acquired via different analytical form due to double wall corrugated cardboard used. Here, no formal finite element analyses were performed to get the crushed shape. Also, the final aim of the computations was not the performance of the single corrugated cardboard sample, but the packaging compressive strength. The numerical study consists of several steps, presented in Figure 6:

- Building the initial geometry of the intact corrugated cardboard (stage a);
- Defining the shape of the crushed corrugated cardboard by a numerical-analytical approximation (stage a-b);
- Building the material stiffness matrix by utilizing the geometry of crushed corrugated cardboard (stage c-d);
- Homogenizing the structure to a single layered composite with a effective properties according to the method presented by Garbowski & Gajewski [23] (stage d-e);
- Computing packaging compressive strength for simple flap boxes with various dimensions by an analytical formula proposed by Garbowski et all. [13] using composite properties acquired in previous stage (stage f);

Intact double-walled corrugated cardboard was assumed as an input geometry to the algorithm. The part of a double wall corrugated cardboard was simulated, namely, the section in plane was 8 × 8 mm. The fluting period for upper layer was 8 mm, the fluting period for lower layer was 4 mm; both fluting layers wave "starts" from the middle of its height. Upper fluting height was equal 4 mm, while lower fluting height was equal 2 mm. The thickness of the liners and fluting papers were 0.29 and 0.30 mm, respectively. The axial spacing between the outer liners was equal 6 mm.

Preprints (www.preprints.org) | NOT PEER-REVIEWED | Posted: 27 May 2021 doi:10.20944/preprints202105.0667.v1

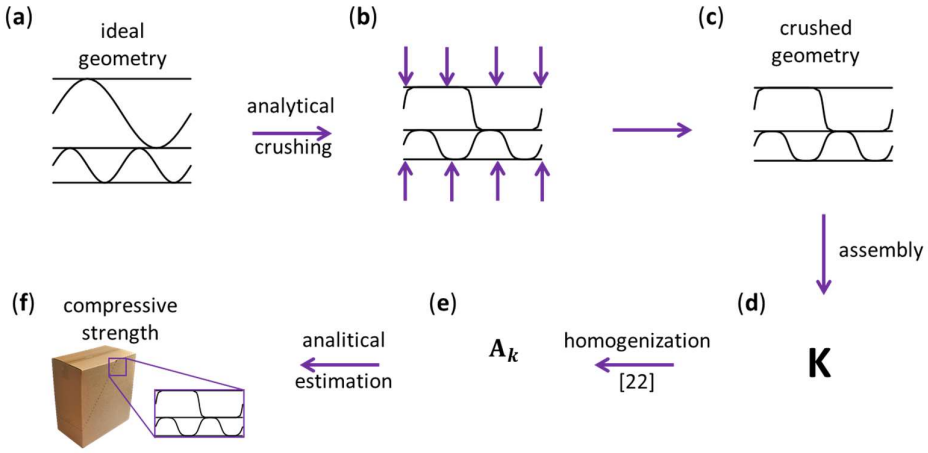

Figure 6. The workflow of the numerical study conducted in this study to determine the packaging compressive strength for crushed corrugated cardboard

The paper materials were modelled by using classical elastic orthotropy. The material data were taken from the literature [16,23,24]. All material data were presented in Table 1, i.e., E_1, E_2, v_{12}, G_{12}, G_{13} and G_{23}, which represents Young moduli in both directions, Poisson's ratio and 3 shear moduli, respectively.

Table 1. Material data of intact double wall corrugated cardboard used for modeling paper layers according to orthotropic constitutive relation.

Layers	E_1 (MPa)	E_2 (MPa)	v_{12} (-)	G_{12} (MPa)	G_{13} (MPa)	G_{23} (MPa)
liners	3326	1694	0.34	859	429.5	429.5
fluting	2614	1532	0.32	724	362	362

In this paper, the crushed geometry of the corrugated cardboard was acquired by simple updated numerical-analytical approach. It should be underlined, that the finite element method computations were not used here. In our previous paper, i.e. [16], both approach (finite element method and analytical) were presented and used equivalently. Here, the updated numerical-analytical approach was only used.

The updated numerical-analytical approach is represented by two components, hyperbolic tangent and linear correction function and reads:

$$y(x) = y_0(x) + ax. \tag{4}$$

The hyperbolic tangent component takes the following form:

$$y_0(x) = \frac{\bar{H}}{2} tanh\left(kx\frac{2\pi}{P}\right), \tag{5}$$

in which $\bar{H}$ is crushed height of the fluting layer, k is crushing parameter found through minimization of the discrepancy between the length of the uncrushed flute and the crushed one (see below), x is the horizontal coordinate along cardboard machine direction, P is the fluting period and a is correction parameter. Parameter a adjusts $y(x)$ for small values of crushing and may be derived by the following relation:

$$a = \frac{\left(\bar{H}/2 - y_0(P/4)\right)}{P/4}. \tag{6}$$

Preprints (www.preprints.org) | NOT PEER-REVIEWED | Posted: 27 May 2021 doi:10.20944/preprints202105.0667.v1

Parameter k is obtained numerically through minimization and it requires length of intact fluting, L, and fluting length of the crushed flute shape, $\bar{L}$:

$$k = \min_{1<k<\infty} (L - \bar{L}). \tag{7}$$

Those length magnitudes, may be computed analytically. Length of intact fluting, L, takes the form:

$$L = \int_{-\frac{P}{4}}^{\frac{P}{4}} \sqrt{1 - \left(\frac{dh}{dx}\right)^2}\, dx. \tag{8}$$

Intact fluting is approximated by sinus function and takes the form:

$$h(x) = \frac{H}{2} \sin\left(x \frac{2\pi}{P}\right) \tag{9}$$

and after derivation one can obtain dh/dx to be used in Equation (8). For a sine-like function, the derivative is:

$$\frac{dh}{dx} = \frac{H\pi}{P} \cos\left(x \frac{2\pi}{P}\right). \tag{10}$$

Length of crushed fluting, $\bar{L}$, takes similar form as in Equation (8):

$$\bar{L} = \int_{-\frac{P}{4}}^{\frac{P}{4}} \sqrt{1 - \left(\frac{dy}{dx}\right)^2}\, dx\,. \tag{11}$$

Explicit form of crushed flute shape function, $y(x)$, reads:

$$y(x) = \frac{\bar{H}}{2} tanh\left(kx \frac{2\pi}{P}\right) + ax \tag{12}$$

and its derivative, dy/dx, takes the following form to be used in Equation (11):

$$\frac{dy}{dx} = -k \frac{\bar{H}\pi}{P} \left(\tanh^2\left(kx \frac{2\pi}{P}\right) - 1\right) + a. \tag{13}$$

Parameters k and a must be computed for particular case of fluting, the input parameters are H and P. As the examples, the parameters k and a were computed for the cardboards with $H = 8$ mm and $P = 4$ mm for various levels of crushing, from 0% to 50% and were presented in Table 2.

Table 2. Exemplary values of k and a parameters for $H = 8$ mm and $P = 4$ mm for different levels of crushing

Crushing level, CRS (%)	k parameter (-)	a parameter (-)
0	1.11	0.0238
5	1.39	0.0091
10	1.68	0.0028
15	2.04	0.0006
20	2.49	0.0001
25	3.13	0
30	4.09	0
35	5.65	0
40	8.58	0
45	15.54	0
50	45.98	0

 doi:10.20944/preprints202105.0667.v1

The discussion above refers to a single fluting layer, however, in this study, the double wall corrugated cardboards are considered. Thus, for each of two fluting layers the crushing distribution must be determined. After experimental observations, the following crushing distribution will be used.

First, let us assume that $H_1 \geq H_2$. Namely, H_1 is the height of higher fluting layer and H_2 is the height of lower fluting height. Further, the crushing level is understood as the following:

$$\bar{t} = t \cdot (100 - CRS)/100, \tag{14}$$

in which t is the total height of intact double wall corrugated cardboard, $\bar{t}$ is its counterpart for crushed double wall corrugated cardboard and CRS is the total crushing level in percentages (considered before elastic relaxation of 50%), e.g. 20 %.

The crushing level of lower fluting, CRS_2, is computed from the following distribution observed experimentally:

$$CRS_2 = CRS \cdot \frac{H_2}{H_1}, \tag{15}$$

in which H_1 is the height of intact higher fluting, while H_2 is the height of intact lower fluting. The height of lower fluting due to crushing, $\bar{H}_2$, takes the following form:

$$\bar{H}_2 = H_2 \cdot (100 - CRS_2)/100. \tag{16}$$

Thus, now we may compute the height of higher fluting due to crushing, $\bar{H}_1$, by simple subtraction:

$$\bar{H}_1 = \bar{t} - \bar{H}_2 \tag{17}$$

and consequently, the crushing level of higher fluting may be accounted by this expression:

$$CRS_1 = \left(1 - \frac{\bar{H}_1}{H_1}\right) \cdot 100\,. \tag{18}$$

Using numerical-analytical approach discussed above to determine the crushing shape of double wall corrugated cardboard, apart intact case (crushing of 0 %), three levels of crushing were assumed for further analyses, namely, 10%, 20% and 30%, see Figure 7. In the first column, the three-dimensional views on the representative volume elements (RVE) were presented, while in the second column the cross-section shapes after crushing were shown. The model of RVE of double wall corrugated cardboard had 1728 shell elements with linear shape functions and 1925 nodes. For representing fluting period, 64 segments were used. Segment analysis was conducted in our recent work [22], it was shown that to obtain the correct transversal shear stiffnesses the number of segments must be large enough. The particular crushing levels for higher and lower fluting obtained from computations (assuming that half of applied CRS recovers due to elastic relaxation) are: 6.25% and 2.5%; 12.5% and 5%; and 18.75% and 7.5% for total creasing of 10%, 20% and 30%, respectively, see Figures 7c-h.

In the next stage of the study, the output geometries (without any residual stresses) were used in finite element preprocessing in-house code to build the material stiffness matrix of the structures analyzed, see Figure 7a,c,e,g. Before this, the deterioration of the material parameter due to delamination was assumed according to [16] – the elastic parameters of selected regions were decreased. The material stiffness matrix of RVEs acquired with embedded orthotropic and locally deteriorated properties (due to decreasing of elastic properties) were processed by the homogenization method of Garbowski &

 doi:10.20944/preprints202105.0667.v1

Gajewski [22]. One of the biggest advantage of the method is the possibility to compute the effective transversal shear stiffness of the input structure. The method enables computing the stiffness matrix of a single laminate shell RVE based on the input structure; here, the corrugated cardboard with different levels of crushing included.

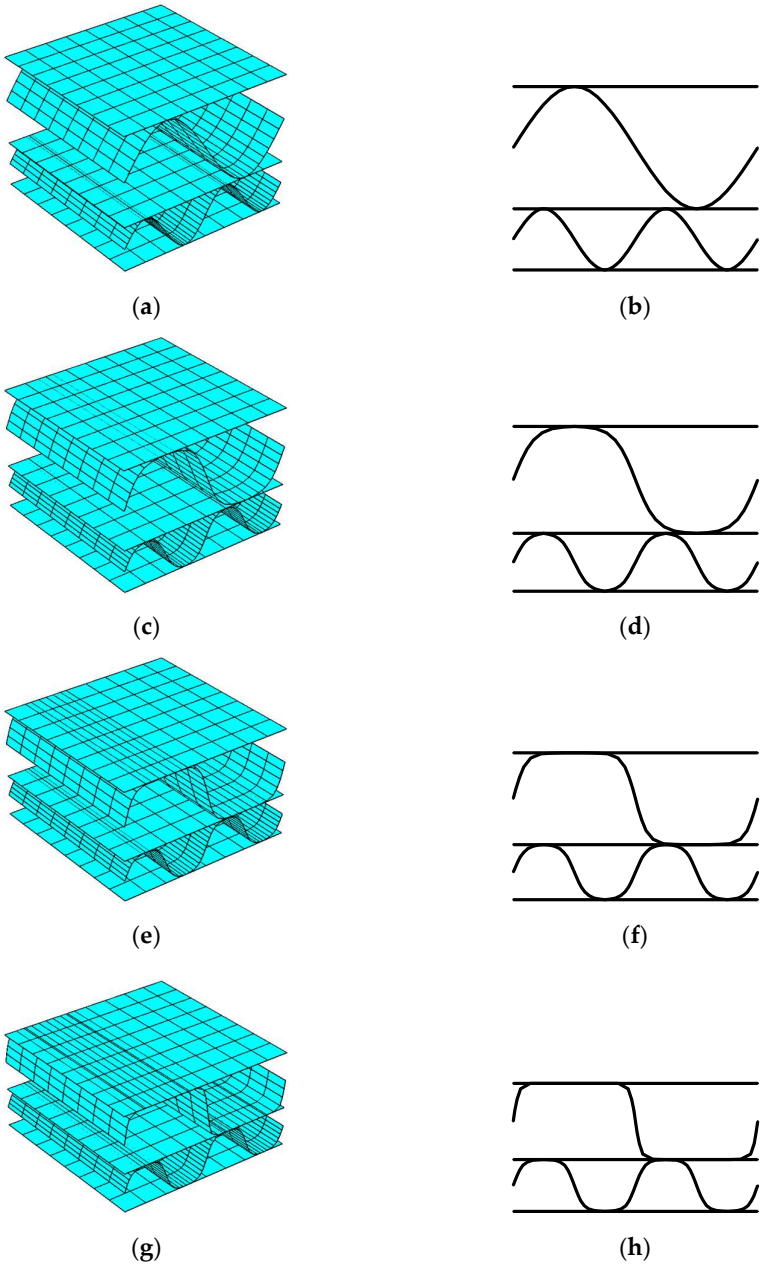

Figure 7. The crushed geometries of double wall cardboard used in the study obtained from the numerical-analytical approach; three-dimensional views (a), (c), (e), (g) and counterpart cross-section shapes (b), (d), (f), (h) for 0%, 10%, 20% and 30%, respectively.

Further, the output data from the homogenization was used to analytically compute the compressive strength of simple flap boxes (with various box dimensions) with different levels of crushing included. The advanced analytical approach was considered, which takes into consideration different box dimensions in plane, material orthotropy and transversal shear stiffnesses. This analytical model was reviewed in details in our previous

Preprints (www.preprints.org) | NOT PEER-REVIEWED | Posted: 27 May 2021 doi:10.20944/preprints202105.0667.v1

work [10]. Thus, only the main formulas are presented here. The compressive strength of the packaging is estimated by the following relation:

$$BCT = 2\bar{k}ECT^{r}[\gamma_b(P_{cr}^{b})^{1-r}b + \gamma_c(P_{cr}^{c})^{1-r}c] \tag{19}$$

in which $\bar{k}$ and r are the dimensionless constants, P_{cr}^{b} and P_{cr}^{c} are the critical forces of box panels of width b and c, respectively; γ_b and γ_c are the reduction coefficients. Critical forces for b and c (box dimensions in plan) are computed according to:

$$P_{cr}^{i} = \frac{M}{N}\frac{1}{\alpha^2}; \quad i = \{b, c\}, \tag{20}$$

in which

$$M = D_{11}\alpha^4 + 2(D_{12} + 2D_{33})\alpha^2\beta^2 + D_{22}\beta^4 + \left(\frac{\alpha^2}{A_{44}} + \frac{\beta^2}{A_{55}}\right)c_1 \tag{21}$$

and

$$N = 1 + \frac{c_1}{A_{44}A_{55}} + \frac{c_2}{A_{55}} + \frac{c_3}{A_{44}}; \quad \alpha = \frac{m\pi}{\bar{a}}; \quad \beta = \frac{\pi}{i}; \tag{22}$$

in which c_1, c_2, c_3 and c_4 are the constants derived from boundary conditions.

ECT value of the cardboard for Equation (19) must be determined in order to compute analytically the compressive strength of the box. Here it was assumed for case study, based on the experiments, to be 8 kN/m. Its decrease due to crushing was computed according the relation observed in our experimental results, see Section 3.1

3. Results

3.1. Experimental study

Four corrugated boards were selected for experimental study; each with a different grammage, exactly two BC flutes: BC-480 (480 g/m^2), BC-580 (580 g/m^2) and two EB flutes: EB-560 (560 g/m^2), EB-670 (670 g/m^2).

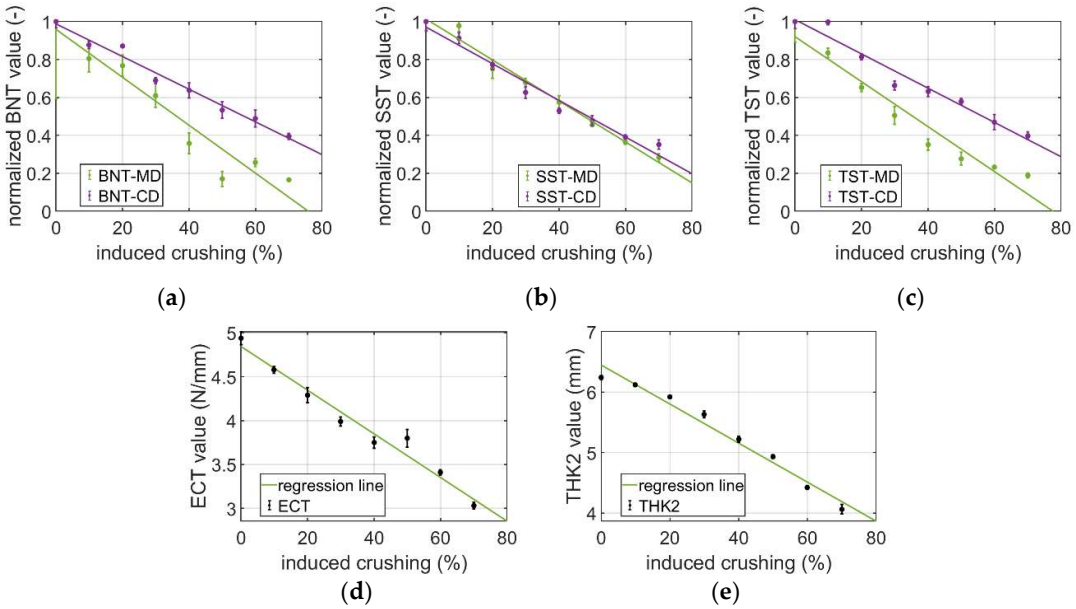

Figure 8. The decreases in measured values for BC-480 double-walled corrugated cardboard in the tests: (a) BNT; (b) SST; (c) TST; (d) ECT; (e) THK2.

Preprints (www.preprints.org) | NOT PEER-REVIEWED | Posted: 27 May 2021 doi:10.20944/preprints202105.0667.v1

The numerous tests and laboratory measurements were carried out on a corrugated boards to verify: (a) bending stiffness in cross-direction (BNT–CD) and in machine direction (BNT–MD); (b) shear stiffness in cross-direction (SST–CD) and in machine direction (SST–MD); (c) torsion stiffness in cross-direction (TST–CD) and in machine direction (TST–MD); (d) sample resistance to edge crushing – ECT; and (e) sample thickness before (intact cardboard) and after crushing – THK2 and THK.

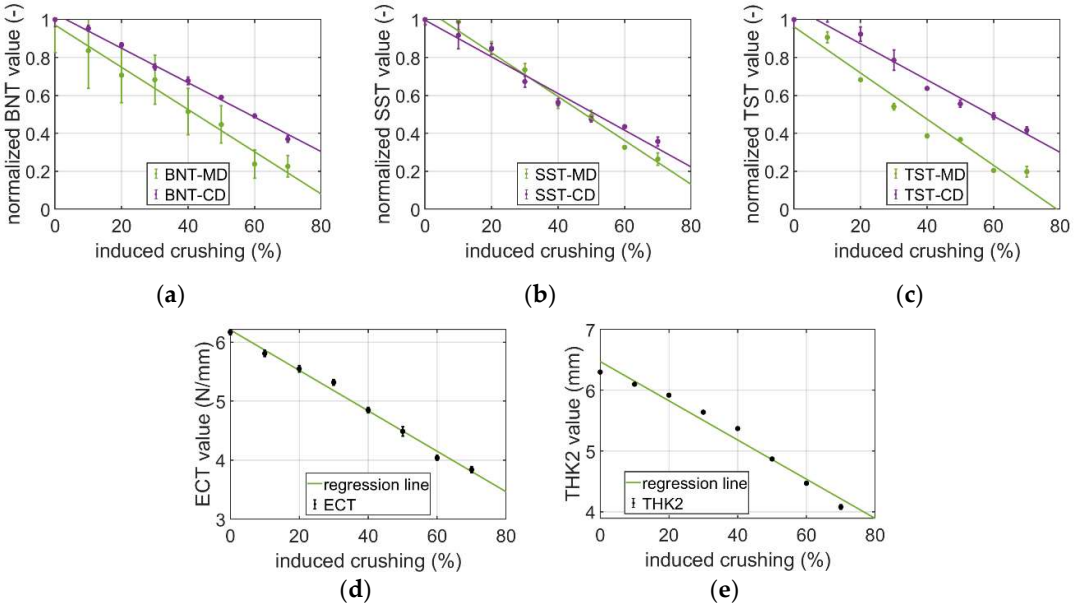

Figure 9. The decreases in measured values for BC-580 double-walled corrugated cardboard in the tests: (a) BNT; (b) SST; (c) TST; (d) ECT; (e) THK2.

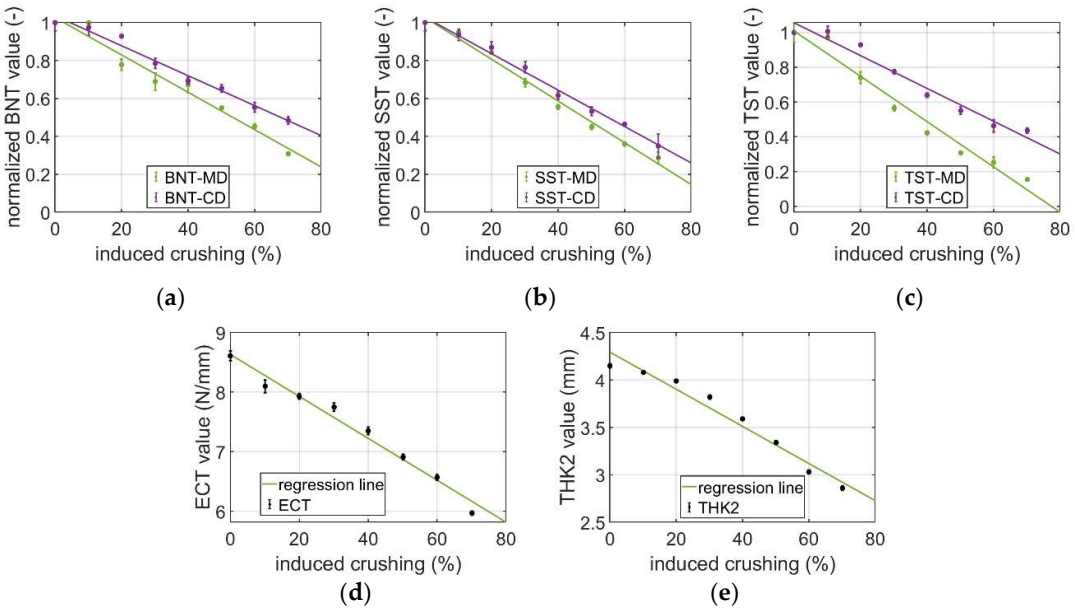

Figure 10. The decreases in measured values for EB-560 double-walled corrugated cardboard in the tests: (a) BNT; (b) SST; (c) TST; (d) ECT; (e) THK2.

Preprints (www.preprints.org) | NOT PEER-REVIEWED | Posted: 27 May 2021 doi:10.20944/preprints202105.0667.v1

Each corrugated cardboard index was subjected to three to five series of tests for the same crushing level. The range of corrugated board crushing was from 10% to 70% of its initial thickness with increments of 10%. The measurement of the thickness of the crushed specimen was carried out several minutes after crushing to take into account the effect of elastic relaxation of corrugated board.Selected results from the laboratory tests are summarized below. In Figures 8-11, the results of different degradation level of the parameters for each of the analyzed double-walled corrugated board are shown. The collection of experimental data enabled computing the regression lines for each test according to Equations (2) and (3). The values of SST, BNT and TST are shown in a standardized way, as the ratio of the value obtained for crushed sample with respect to the initial value (i.e. for CRS = 0%).

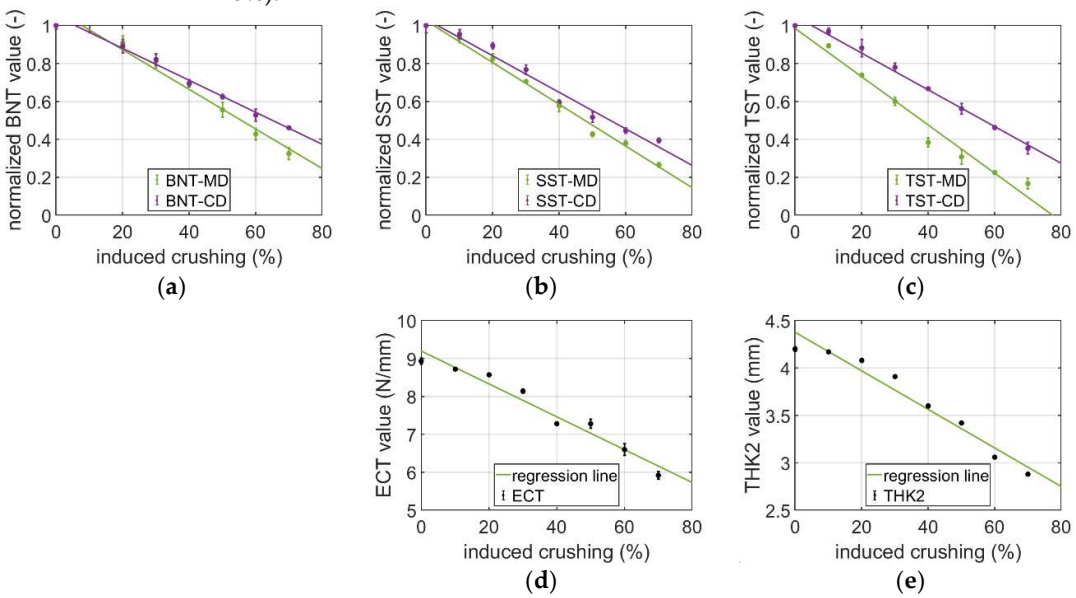

Figure 11. The decreases in measured values for EB-670 double-walled corrugated cardboard in the tests: (a) BNT; (b) SST; (c) TST; (d) ECT; (e) THK2.

In order to determine the relationship between crushing and the deterioration of measured mechanical parameters of double-walled corrugated board, the coefficient of determination for each quantity was computed according to Equation (1). The values obtained are summarized in Table 3.

Table 3. The coefficient of determination R^2 for all corrugated cardboards considered and different measurements.

Cardboard index	THK2	ECT	BNT-MD	BNT-CD	SST-MD	SST-CD	TST-MD	TST-CD
BC-480	0.000	0.302	0.591	0.956	0.989	0.993	0.566	0.954
BC-580	0.014	0.304	0.898	0.917	0.976	0.998	0.704	0.877
EB-560	0.000	0.000	0.981	0.727	0.989	0.965	0.726	0.888
EB-670	0.000	0.000	0.915	0.770	0.988	0.957	0.695	0.931

Using the mean value of the measured parameters in both cross-machine direction (CD) and machine direction (MD) to calculate the linear regression is more accurate. Figure 12 represents the crushing line and the normalized parameter values averaged from two directions. The coefficients of determination for averaged values from two directions are shown in Table 4.

Preprints (www.preprints.org) | NOT PEER-REVIEWED | Posted: 27 May 2021 doi:10.20944/preprints202105.0667.v1

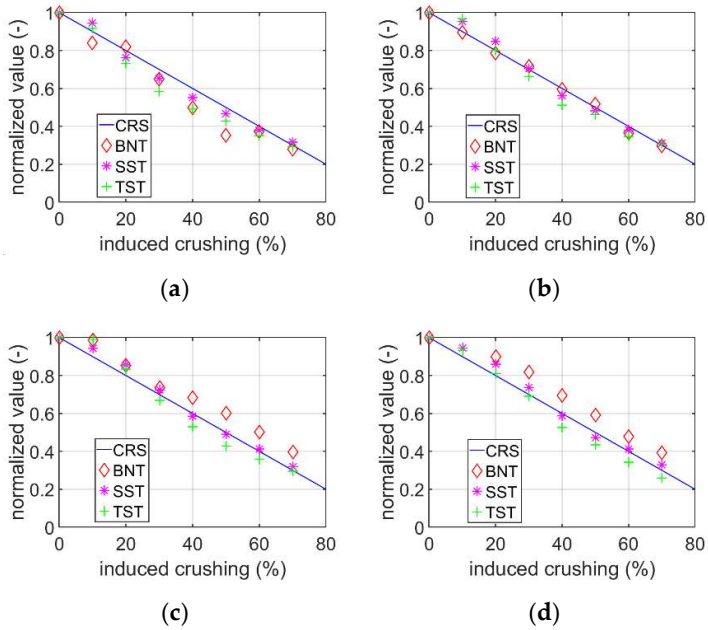

Figure 12. The decreases in measured parameters (average from two directions data) for double-walled corrugated cardboards: (a) BC-480; (b) BC-580; (c) EB-560; (d) EB-670.

Table 4. The coefficient of determination R^2 due to averaging data in double direction tests for all corrugated cardboards considered.

Cardboard index	BNT	SST	TST
BC-480	0.951	0.995	0.949
BC-580	1.000	0.996	0.987
EB-560	0.892	0.994	0.982
EB-670	0.859	0.993	0.974

Values of ECT and THK2 obtained from the measurements show similar trends, this is visible for all types of the samples. Thus, a reference line was adopted to describe the relationship between the deterioration of normalized parameters: ECT and THK2 and the level of crushing of the double-walled corrugated board. The reference line equation takes the following form:

$$y = 1 - 0.46x \tag{23}$$

where: x – the crushing value and y – the normalized parameter value.

In Figure 13, the fittings of the reference line computed from Equation (23) to the normalized data of ECT and THK2 for the analysed corrugated cardboards are shown. It is worth noting that all experimental data can be approximated (with high accuracy) by linear functions, which makes it much easier to infer and build equivalent models in the next step.

The coefficients of determination R^2 were also calculated for the reference line and normalized ECT and THK2 values according to Equation (1), see Table 5. In Equation (1), x_i is reference line value calculated from the Equation (23), $\hat{y}_i$ is normalized THK2 and ECT values, and $\mathrm{var}(x)$ is variance of the reference line value.

Preprints (www.preprints.org) | NOT PEER-REVIEWED | Posted: 27 May 2021 doi:10.20944/preprints202105.0667.v1

Table 5. The values of coefficient of determination R^2 between reference line and normalized ECT and THK2 quality.

Cardboard index	R^2
BC-480	0.977
BC-580	0.967
EB-560	0.941
EB-670	0.930

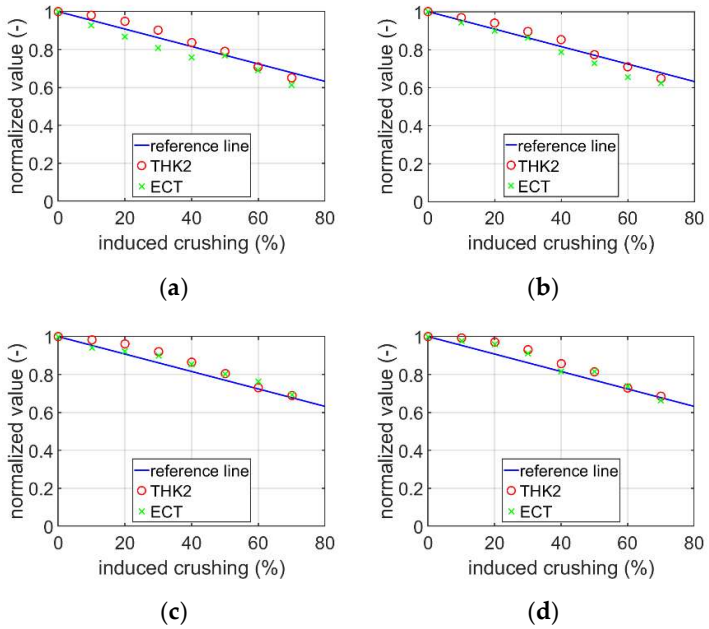

Figure 13. The decreases in normalized THK2 and ECT values for double-walled corrugated cardboard with an index of: (a) BC-480; (b) BC-580; (c) EB-560; (d) EB-670.

3.2 Modelling crushing in estimating compressive strength of packaging

The laminate shell stiffnesses were computed for three crushing levels of corrugated cardboard, in which the crushing levels were 10%, 20% and 30%, but also for the intact cardboard (0% of crushing). Selected values of the stiffnesses computed, required to estimate the compressive stiffnesses of the packaging according to Equation (19), are presented in Table 6. Also, the values of ECT computed according to Equation (23) for different levels of crushing are presented in the same table in the last row.

Table 6. The computed stiffnesses of the representative shell element computed for different levels of crushing of double wall corrugated cardboard.

	0% crushing	10% crushing	20% crushing	30% crushing
D_{11}, (Pa · m^3)	19514	17598	15751	14006
D_{22}, (Pa · m^3)	14326	12759	11273	9876
D_{12}, (Pa · m^3)	3438	3094	2763	2453
D_{33}, (Pa · m^3)	5629	5069	4517	3993
A_{44},(Pa · m)	77.3	52.1	39.5	30.5
A_{55}, (Pa · m)	237.0	211.7	187.6	164.7
ECT (kN/m)	8.0	7.6	7.2	6.8

 doi:10.20944/preprints202105.0667.v1

The main aim of the numerical part of the study was to check what is the influence of the particular level of crushing for double wall corrugated cardboard packaging on its compressive strength. Therefore, varied dimensions of large corrugated cardboard boxes were selected and computed according to the analytical approach presented in Equation (19). Typical flap boxes were analyzed. The boxes dimensions from 500 mm to 1000 mm were assumed to obtain the following ratios of box dimensions in plan: 1:1, 1:2, 1:3, 1:4, 1:5 and 2:3. Three heights of the boxes were considered, i.e., 500 mm, 750 mm and 1000 mm. The input data of boxes dimensions and the compressive strength for different levels of crushing are presented in Table 7.

Table 7. The dimensions of the boxes considered in the numerical study of the paper and the resulted compressive box strength for different level of crushing.

box dimensions			box compressive strength due to crushed cardboard			
b (mm)	c (mm)	a (mm)	0% (N)	10% (N)	20% (N)	30% (N)
500	500	500	6001	5613	5227	4848
500	1000	500	6933	6490	6049	5616
300	900	500	5805	5433	5064	4701
250	1000	500	5894	5516	5141	4772
200	1000	500	5685	5320	4958	4602
600	900	500	7132	6676	6223	5777
500	500	750	6177	5773	5373	4979
500	1000	750	6469	6052	5638	5230
300	900	750	5378	5031	4686	4347
250	1000	750	5367	5021	4679	4341
200	1000	750	5156	4824	4494	4170
600	900	750	6686	6256	5828	5406
500	500	1000	6001	5613	5227	4848
500	1000	1000	6257	5854	5453	5059
300	900	1000	5295	4952	4611	4276
250	1000	1000	5218	4880	4545	4215
200	1000	1000	5004	4680	4358	4042
600	900	1000	6646	6218	5793	5373

4. Discussion

In the experimental part of this research, the relation between intentionally induced crushing (CRS) of the double wall corrugated cardboard and the output from the mechanical laboratory tests of the cardboard was studied, see Figures 8-11. Four types of fluting compositions of double wall corrugated cardboards were analyzed, two BC and two EB cardboards. The coefficients of determination were computed for all measurements, namely, thickness, ECT, bending (BNT), shearing (SST) and twisting (TST), the later three in CD and MD, see Table 3–5. The highest determination ratios were obtained for corrugated cardboard of BC-580. If the mean values from CD and MD are considered the highest determination ratios were observed in SST (0.995) in comparison to BNT (0.926) and TST (0.973). This means that SST is able to predict crushing of the cardboard best in our crushing controlled experimental study. Similar conclusions were obtained for single wall corrugated cardboards [16]. Regression lines were also computed for each measurement type, see Figure 12–13. For ECT and thickness measurements the reference line equation was derived, from which it may be concluded that the particular percentage level of crushing drops those magnitudes of ECT and thickness measured with 46% of crushing level.

 doi:10.20944/preprints202105.0667.v1

In the numerical part of the study the intact and crushed cardboard was investigated, in particular the decrease of its laminate stiffnesses properties and the decrease of the packaging compressive strength. It appeared that, for instance, if one compare the intact cardboard (0% crushing) and 30% crushing case the decreases in almost all effective stiffnesses are about 29%, see Table 6. Only for A_{44} the decrease is about twice bigger, i.e. 61%. Similar outcome was obtained for 10% and 20% of crushing, but the drops are proportionally lower.

The packaging compressive strengths were presented in Table 7. It may be observed that the values of compressive strength for intact corrugated cardboard (0% of crushing) are between about 5000 N and 7100 N. The values for 10% of crushing are between 4700 N and 6700 N. The values for 20% of crushing are between 4400 N and 6200 N. The values for 30% of crushing are between 4000 N and 5800 N. The results for crushing of 10%, 20% and 30% referred to the results for intact corrugated cardboard packaging gives almost the same percentage differences if one consider row to row values, i.e. between different box dimensions. Concluding, the drop in compressive strength of the packaging due to crushing is not sensitive to box dimensions.

Further, the results show that if one compares the results for box with intact corrugated cardboard and with the crushed one with 10%, 20% and 30%, the percentage differences are 6.4%, 12.8% and 19.1%, respectively. For instance, in the last case, namely, 600 mm x 900 mm x 1000 mm box, the compressive strength of the packaging with intact corrugated cardboard is 6646 N; the compressive strength of the packaging with the same cardboard, but crushed with 30% equals 5373 N – the percentage difference for those values is 19.2%. Notice that the relation between crushing level and percentage drop is almost linear, and may be approximated by the factor of $16/25$. For instance, if the crushing is equal 25%, the drop in packaging compressive strength would be $25\% \cdot 16/25 = 16\%$.

The numerical modelling presented may be used for estimating the influence of the crushed corrugated cardboard on the packaging compressive strength for cardboards with other shapes of fluting without the use of finite element analysis based on the precise crushing estimation by shear stiffness test.

5. Conclusions

In this work, a series of mechanical tests were carried out on various double-walled corrugated cardboards. In these tests, the effect of intentional and fully controlled crushing introduced into the samples in the range from 10 to 70% was checked. Based on experimental observations, an analytical crush model was proposed and then homogenized using the RVE finite element stiffness matrix and techniques and strain equivalence approach. Ultimately homogenized, crushed corrugated cardboard samples were used in a theoretical case study to understand the effect of a certain level of crush on the performance of the different flap boxes. It was observed that there are simple linear relationships between the deteriorating measured values and the amount of crush, a similar relationship was observed between the load-bearing capacity of the selected flap boxes and the degree of crushing of the corrugated cardboard.

Author Contributions: Conceptualization, T.Gar.; methodology, T.Gar.; software, T.Gar. T.Gaj.; validation, T.Gar., T.Gaj., N.S.; formal analysis, T.Gar. T.Gaj., N.S.; investigation, T.Gar., T.Gaj., N.S. P.W.; writing—original draft preparation, T.Gar., T.Gaj., N.S.; writing—review and editing, T.Gar., T.Gaj., M.K.; visualization, T.Gaj., T.Gar. and N.S.; supervision, T.Gar. ; project administration, T.Gar.; funding acquisition, M.K.

Funding: The APC was funded by the National Center for Research and Development, Poland, grant at Schumacher Packaging Sp. z o. o., grant number POIR.01.01.01-00-1006/19.

Data Availability Statement: The data presented in this study are available on request from the corresponding author.

Acknowledgments: The authors thank AQUILA VPK Wrzesnia for providing samples of corrugated cardboard for the study. The authors also thank to Femat Sp. z o. o. for providing the laboratory equipment.

Conflicts of Interest: The authors declare no conflicts of interest. The funders had no role in the design of the study; in the collection, analyses, or interpretation of data; in the writing of the manuscript, or in the decision to publish the results.

References

1. Garbowski T, Gajewski T, Grabski JK. Estimation of the Compressive Strength of Corrugated Cardboard Boxes with Various Openings. Energies. 2021; 14(1):155. https://doi.org/10.3390/en14010155
2. Fadiji, T.; Ambaw, A.; Coetzee, C.J.; Berry, T.M.; Opara, U.L. Application of the finite element analysis to predict the mechanical 490 strength of ventilated corrugated paperboard packaging for handling fresh produce. Biosyst. Eng. 2018, 174, 260–281.
3. Garbowski T, Gajewski T, Grabski JK. Estimation of the Compressive Strength of Corrugated Cardboard Boxes with Various Perforations. Energies. 2021; 14(4):1095. https://doi.org/10.3390/en14041095
4. Gallo, J.; Cortés, F.; Alberdi, E.; Goti, A. Mechanical Behavior Modeling of Containers and Octabins Made of Corrugated Cardboard Subjected to Vertical Stacking Loads. Materials 2021, 14, 2392. https://doi.org/10.3390/ma14092392
5. Shick, P.E.; Chari, N.C.S. Top-to-bottom compression for double wall corrugated boxes. Tappi J. 1965, 48, 423–430.
6. McKee, R.C.; Gander, J.W.; Wachuta, J.R. Compression strength formula for corrugated boxes. Paperboard Packag. 1963, 48, 149– 159.
7. Batelka, J.J.; Smith, C.N. Package Compression Model; Institute of Paper Science and Technology: Atlanta, GA, USA, 1993.
8. Urbanik, T.J.; Frank. B. Box compression analysis of world-wide data spanning 46 years. Wood Fiber Sci. 2006, 38, 399–416.
9. Ristinmaa, M.; Ottosen, N.S.; Korin, C. Analytical Prediction of Package Collapse Loads-Basic considerations. Nord. Pulp Pap. Res. J. 2012, 27, 806–813.
10. Garbowski. T.; Gajewski. T.; Grabski. J.K. The role of buckling in the estimation of compressive strength of corrugated cardboard boxes. Materials 2020, 13, 4578. https://doi.org/10.3390/ma13204578
11. Schrampfer, K.E.; Whitsitt, W.J.; Baum, G.A. Combined Board Edge Crush (ECT) Technology; Institute of Paper Chemistry: 476 Appleton, WI, USA, 1987.
12. Garbowski T, Gajewski T, Grabski JK. Torsional and Transversal Stiffness of Orthotropic Sandwich Panels. Materials. 2020; 13(21):5016. https://doi.org/10.3390/ma13215016
13. Garbowski, T.; Gajewski, T.; Grabski, J.K. Role of transverse shear modulus in the performance of corrugated materials. Materials 2020, 13, 3791. https://doi.org/10.3390/ma13173791
14. Popil, R.E.; Coffin, D.W.; Habeger, C.C. Transverse shear measurement for corrugated board and its significance. Appita, J. 2008, 61, 307–312.
15. Nordstrand, T.; Carlssoon, L.A. Evaluation of transverse shear stiffness of structural core sandwich plates. Comp. Struct. 1997, 37, 145–153.
16. Garbowski, T.; Gajewski, T.; Mrówczyński, D.; Jędrzejczak, R. Crushing of Single-Walled Corrugated Board During Converting: Experimental and Numerical Study. Preprints 2021, 2021050403 (doi: 10.20944/preprints202105.0403.v1).
17. Jamsari MA, Kueh C, Gray-Stuart EM, Dahm K, Bronlund JE. Modelling the impact of crushing on the strength performance of corrugated fibreboard. Packag Technol Sci. 2020;33:159–170. https://doi.org/10.1002/pts.2494
18. Jamsari MA, Kueh C, Gray-Stuart E, Martinez-Hermosilla GA, Dahm K, Bronlund JE. A technique to quantify morphological damage of the flute profile in the midplane of corrugated fibreboard. Packag Technol Sci. 2019;32:213–226. https://doi.org/10.1002/pts.2431
19. Martinez-Hermosilla GA, Kueh C,Dahm K, Bronlund JE. Combined modelling methodology for opti-misation of box design based on hybrid genetic algorithm. PackagTechnol Sci. 2018;31:709–722.https://doi.org/10.1002/pts.2410
20. Berry TM, Fadji TS, Defraeyea T, Opara UL. The role of horticulturalcarton vent hole design on cooling efficiency and compressionstrength: a multi-parameter approach. Postharvest Biol Technol.2017;124:62-7
21. FEMat Systems - BSE. Available online: http://fematsystems.pl/bse-system_en/ (online access on 15th of May 2021).
22. FEMat Systems - CRS. Available online: http://fematsystems.pl/crs_en/ (online access on 15th of May 2021).
23. Garbowski, T.; Gajewski, T. Determination of transverse shear stiffness of sandwich panels with a corrugated core by numerical homogenization, Materials 2021, 14 1976. https://doi.org/10.3390/ma14081976
24. Biancolini, M.E. Evaluation of equivalent stiffness properties of corrugated board. Compos. Struct. 2005, 69, 322–328. 495